

Supporting Information

Monodisperse Tin Nanoparticles and Hollow Tin Oxide Nanospheres as Anode Materials for High Performance Lithium Ion Batteries

Xixia Zhao,^{a,b‡} Wenhui Wang,^{b‡} Zhen Hou,^b Yikang Yu,^b Qian Di,^{a,b}
Xiaotong Wu,^b Guijuan Wei,^a Zewei Quan^{*b} and Jun Zhang^{*a}

^aState Key Laboratory of Heavy Oil Processing, College of Chemical Engineering, China University of Petroleum, Qingdao, Shandong 266580, P. R. China. E-mail: zhangj@upc.edu.cn

^bDepartment of Chemistry, Southern University of Science and Technology (SUSTech), Shenzhen, Guangdong 518055, P. R. China. E-mail: quanzw@sustc.edu.cn

[‡]These authors contributed equally to this work.

Experimental Section

Chemicals: Tin (II) chloride (SnCl_2 , 99%) and hexacarbonyl tungsten ($\text{W}(\text{CO})_6$, 97%) were purchased from Alfa Aesar. Hexamethyldisilazane (HMDS, 99%), oleylamine (OAm, 70%), and 1-octadecene (ODE, 90%) were purchased from Aldrich. OAm and ODE were dried under vacuum at 120 °C for 1 h and then stored under an Ar atmosphere prior to use. All other reagents were used as received.

Synthesis of Sn nanoparticles: Monodisperse Sn nanoparticles were synthesized in large quantity by a modified method based on our previous recipe.¹ Typically, SnCl_2 (0.4 g), $\text{W}(\text{CO})_6$ (0.1 g), HMDS (0.75 mL), OAm (10 mL) and ODE (90 mL) were mixed in a three-neck flask under the protection of Ar flow. The mixture was firstly heated to 60°C and kept at this temperature for 10 min, then heated to 210 °C at a rate of 10 °C min^{-1} . The solution turned to brown black when up to 210 °C and held for 20 min. After cooled down to room temperature, the product was separated and purified three times by adding hexane/ethanol through centrifugation.

Synthesis of hollow SnO_x nanospheres: Typically, SnCl_2 (0.4 g), $\text{W}(\text{CO})_6$ (0.1 g), HMDS (0.75 mL), OAm (10 mL), and ODE (90 mL) were mixed in a three-neck flask under the protection of Ar flow. The mixture was firstly heated to 60 °C and kept at this temperature for 10

min, then heated to 210 °C at a rate of 10 °C min⁻¹. The solution turned to brown black when up to 210 °C and held for 20 min. After cooled down to room temperature, the solution was degassed until no bubbles were generated. After filling air into the flask, the mixture was heated to 180 °C and held for 30 min. After cooled down to room temperature, the product was separated and purified three times by adding hexane/ethanol through centrifugation.

Ligand removal: The as-prepared product (Sn nanoparticles or hollow SnO_x nanospheres) was dispersed in n-butylamine (the weight ratio of solid to liquid is about 1:120) and stirred for at least 12 h, and then was separated and purified several times by adding hexane/ethanol through centrifugation. At last, powder was obtained by drying the sediment under vacuum at 60 °C for at least 2 h.

Characterizations: X-ray diffraction (XRD) patterns were recorded on an X-ray diffractometer (Rigaku SmartLab) with Cu K α radiation ($\lambda = 0.15418$ nm) at a voltage of 45 kV and a current of 200 mA. Transmission electron microscope (TEM) images and elemental mapping were obtained using FEI Tecnai F30 electron microscope (300 kV). TEM samples were prepared by placing a drop of the nanoparticle colloidal solution onto a carbon-coated Cu grid under ambient conditions. The elements on the surface of these nanoparticles were determined by X-ray photoelectron spectroscopy (XPS, PHI 5000 VersaProbe II).

Electrochemical measurements: The electrochemical performance of two materials was assessed into CR2032 coin-type cell using 16 mm Li disc as counter/reference electrode. The working electrode casted on Ti foil was consists of the as-prepared powder, carbon black (Super P) and carboxymethyl cellulose (CMC) in a weight ratio of 6:2:2. The casted electrode was nature dried for 1 h followed by vacuum dried at 60 °C overnight. **The working electrode is a disc with diameter of 16 mm and the typical loading of active materials is $\sim 1.0 \text{ mg cm}^{-2}$.** The separator is Celgard2325 and the electrolyte is 1.0 M LiPF_6 in a 1:1:1 (v/v/v) mixture of ethylene carbonate, ethyl methyl carbonate, and dimethyl carbonate. The discharge–charge test was conducted using a Neware battery testing system under different rates within an operating voltage window of 0.01–2.0 V (vs. Li/Li^+). The specific capacity was calculated based on the mass of the active material. The CV was performed within a voltage window of 0.01–2.0 V at a scan rate of 0.1 mV s^{-1} . All tests were conducted at room temperature unless otherwise specified.

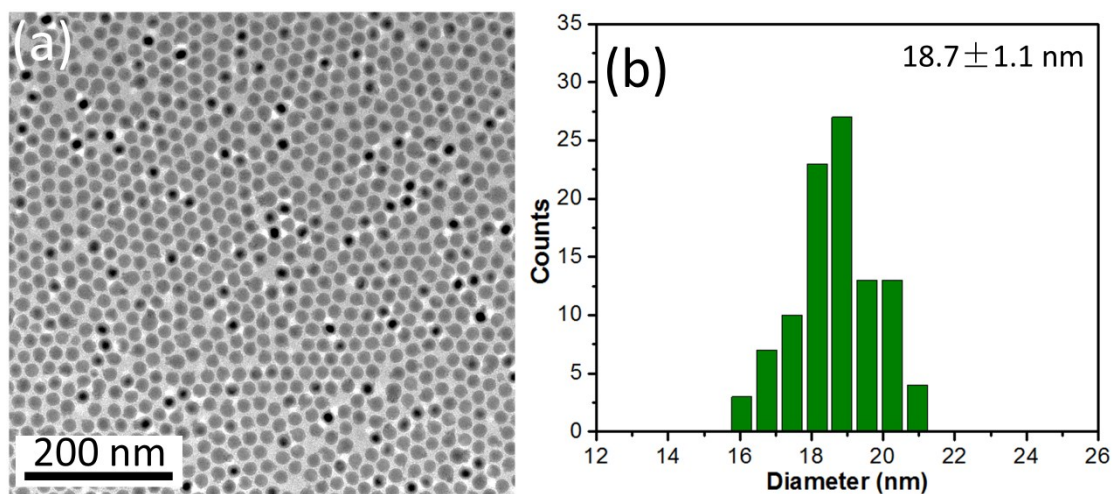


Fig. S1 TEM image (a) and corresponding size distribution (b) based on statistics collected over 250 particles of as-prepared Sn nanoparticles.

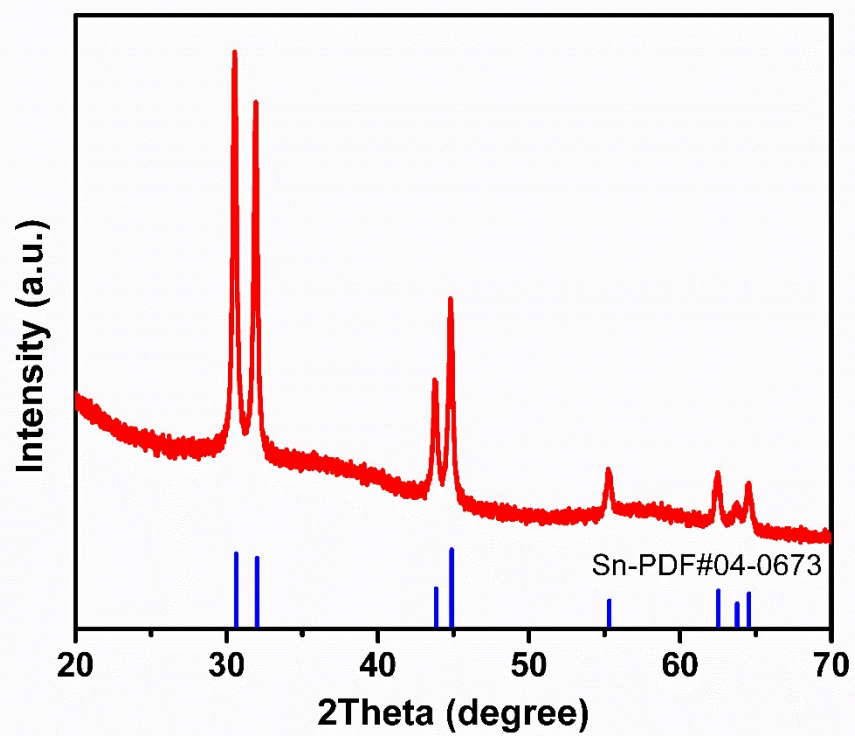


Fig. S2 XRD pattern of as-prepared Sn nanoparticles.

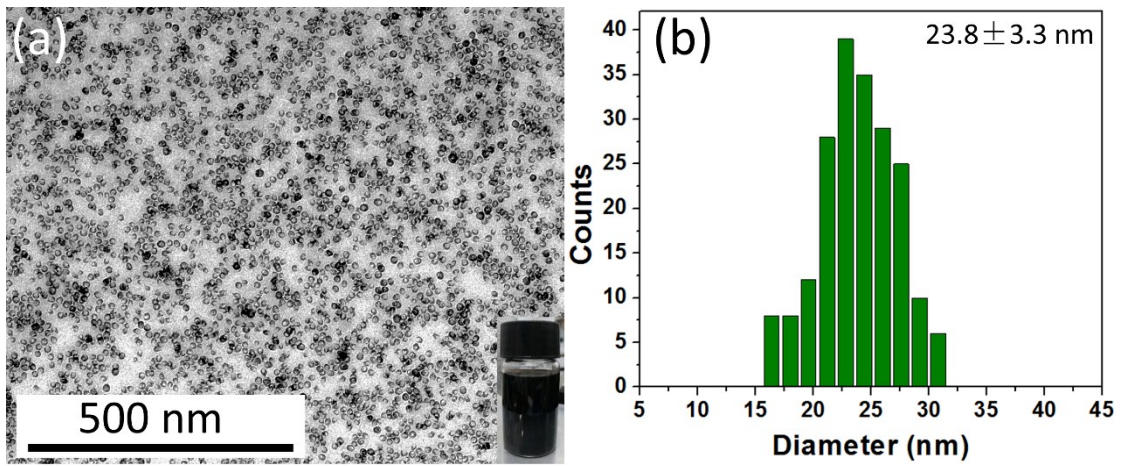


Fig. S3 TEM image (a) and corresponding size distribution (b) based on statistics collected over 200 particles of as-prepared hollow SnO_x nanospheres.

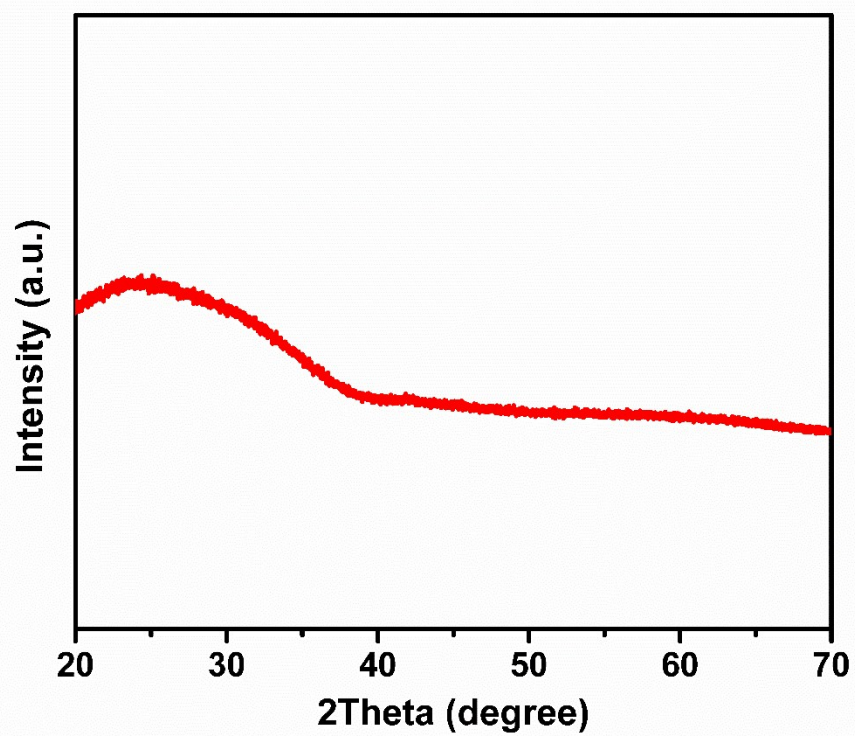


Fig. S4 XRD pattern of as-prepared hollow SnO_x nanospheres.

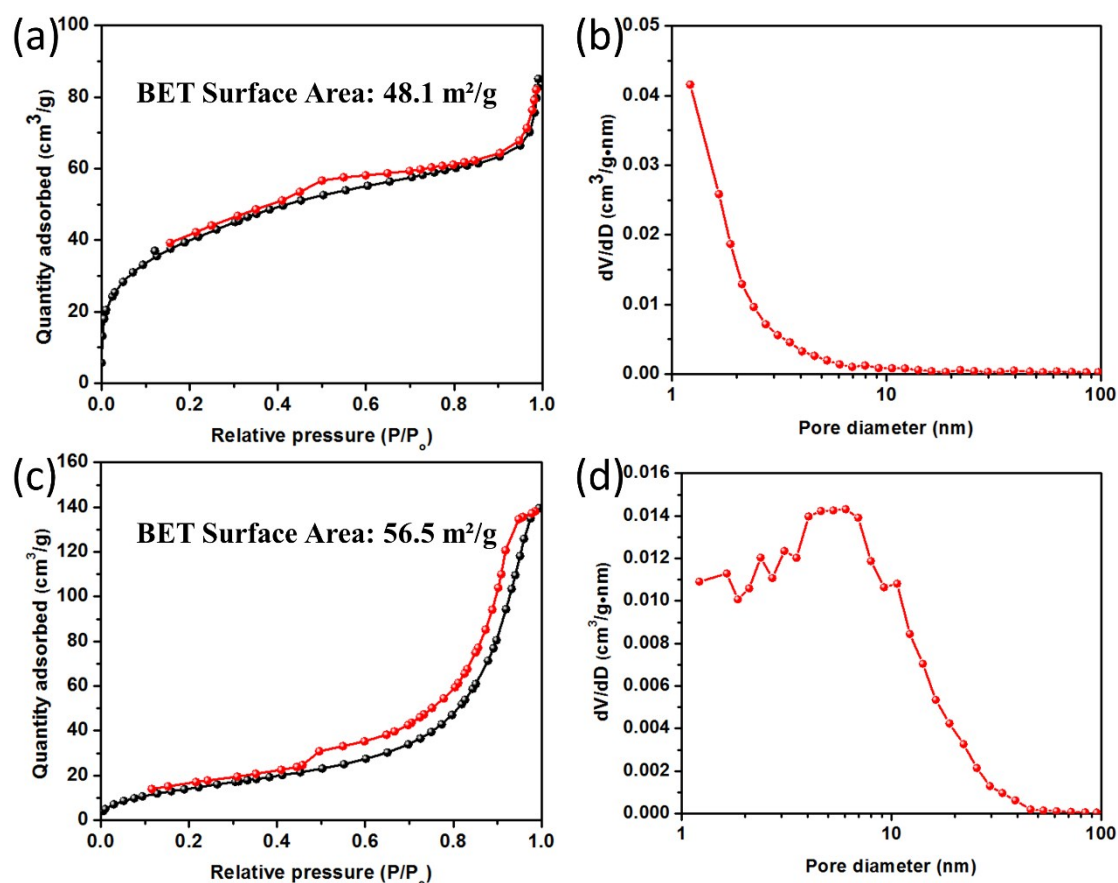


Fig. S5 N₂ gas adsorption and desorption isotherm and pore size distribution of as-prepared (a and b) Sn nanoparticles and (c and d) hollow SnO_x nanospheres.

The porous properties of the Sn nanoparticles and hollow SnO_x nanospheres were determined by N₂ adsorption/desorption experiments (Fig. S5). The shape of the isotherm gives a qualitative assessment of the porous structure of these materials. The isotherms of both samples exhibit hysteresis loops of mesoporous materials. The corresponding pore size distribution curves are also calculated from the adsorption branch of isotherms by the BJH method. Hollow SnO_x nanospheres exhibit a larger BET specific surface area of ~56.5 m²/g as compared to that of the Sn nanoparticles (~48.1 m²/g).

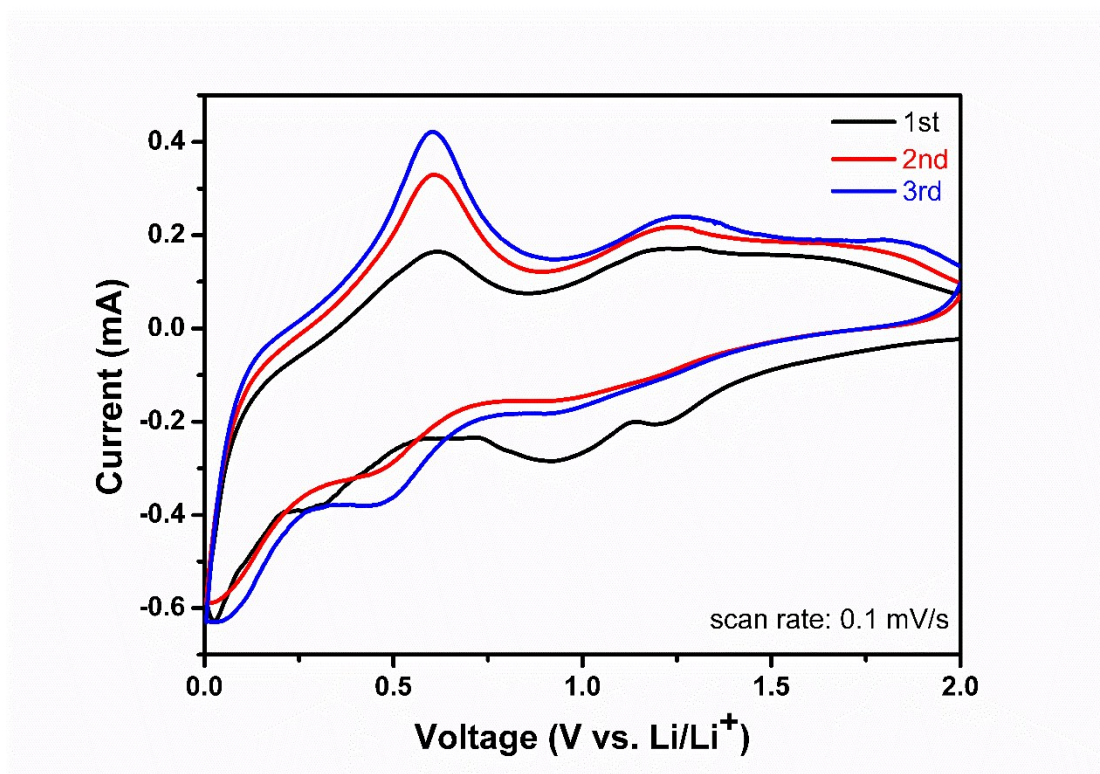


Fig. S6 CV curves of as-prepared Sn nanoparticles anode recorded with a scan rate of 0.1 mV/s.

The electrochemical reactions were investigated by cyclic voltammetry (CV) measurement at the scan rate of 0.1 mV/s and the results are shown in Fig. S5. For cathodic scan, an irreversible peak observed at ~ 1.2 V corresponds to SEI layer formation and a broad peak at ~ 0.9 V is ascribed to the conversion reaction of tin oxide layer to Sn and Li_2O . The remaining peaks in the voltage range of ~ 0.6 to 0 V corresponds to stepwise alloying to $\text{Li}_{4.4}\text{Sn}$ alloy. In the first anodic scan, the peak at ~ 0.6 V is due to dealloying reaction from $\text{Li}_{4.4}\text{Sn}$ to Sn and a broad peak at 1.2 V is attributed to the partial oxidation reaction of Sn to SnO_x on the surface of the electrode.² On one hand, the CV curves persist to show similar features except for first cathodic scan, suggesting the similar electrochemistry process. On the other hand, the current densities of the alloying/dealloying reaction redox peaks raise gradually upon extended cycles, which can be ascribed to the gradual removal of the trace amounts of inert ligands (e.g., OAm) on Sn nanoparticle surface during first few cycles.

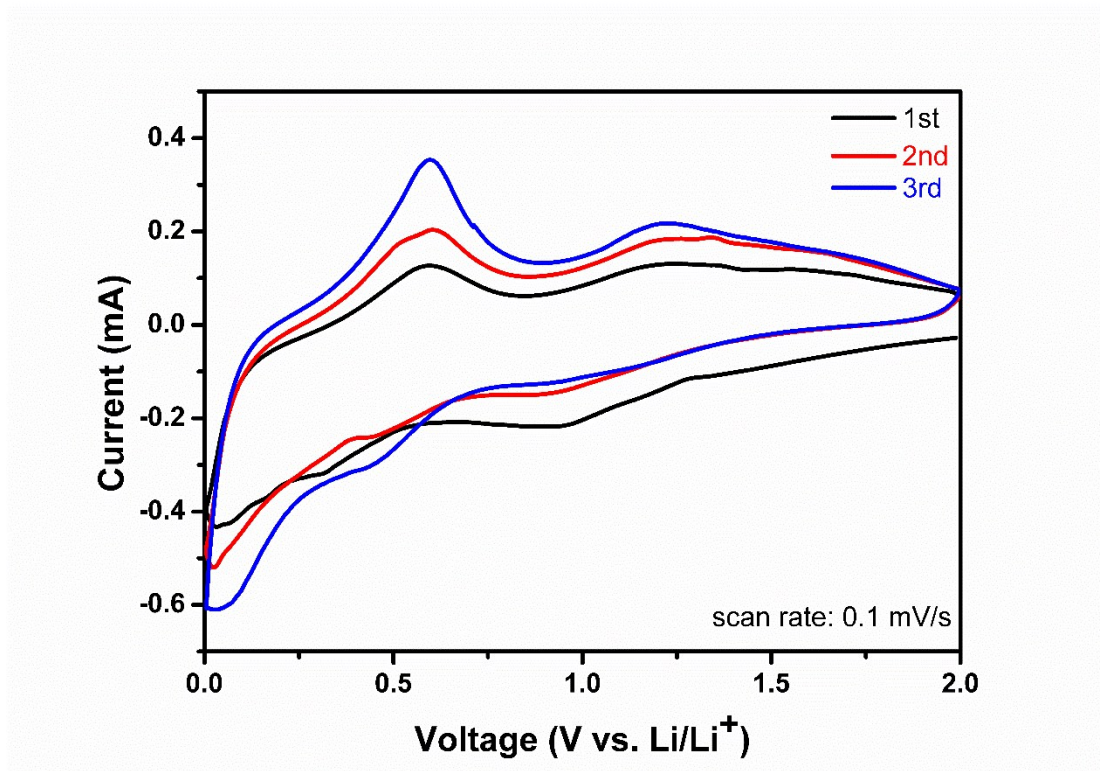


Fig. S7 CV curves of as-prepared hollow SnO_x nanospheres anode recorded with a scan rate of 0.1 mV/s.

Fig. S6 shows the initial three cycles with a voltage range of 0.01~2.0 V at a scan rate of 0.1 mV/s. For cathodic scan, the broad peak at around 0.5–1.2 V is mainly due to the formation of the SEI layer and the conversion reaction of SnO₂ to Sn and Li₂O. The remaining peaks in the voltage range of 0.5-0.2 V correspond to the Li_{4.4}Sn alloy formation reaction. In the first anodic scan, peaks at ~0.6 V and 1.2 V can be attributed to dealloying reaction from Li_{4.4}Sn to Sn and partial oxidation reaction of Sn to SnO_x on the surface of the electrode, respectively.

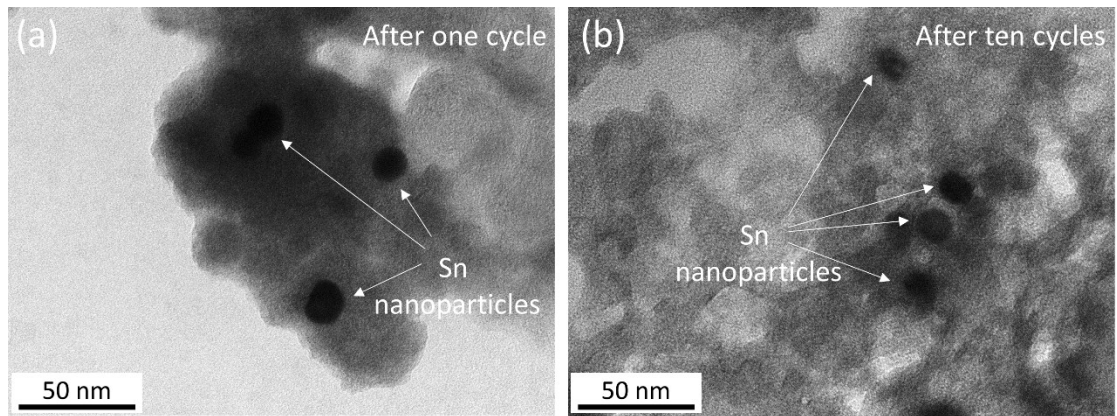


Fig. S8 TEM images of as-prepared Sn nanoparticles (a) after one cycle and (b) after ten cycles at a current density of 500 mA/g.

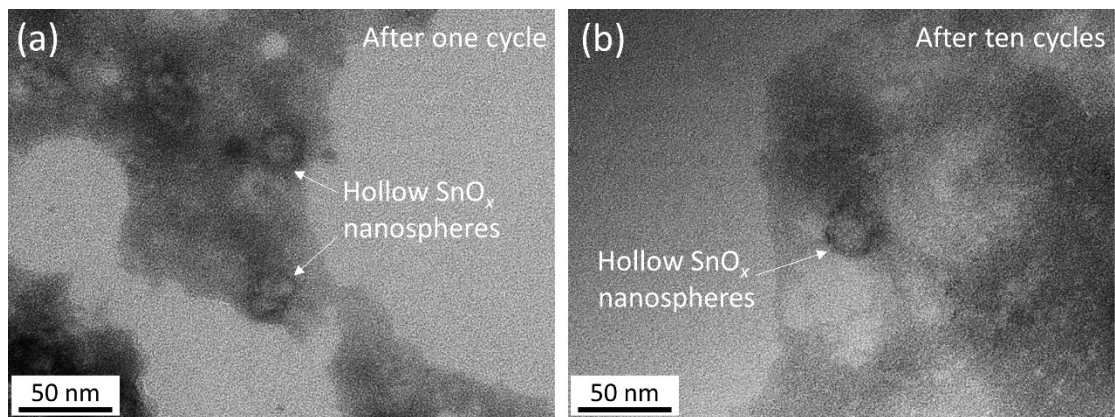


Fig. S9 TEM images of as-prepared hollow SnO_x nanospheres (a) after one cycle and (b) after ten cycles at a current density of 500 mA/g.

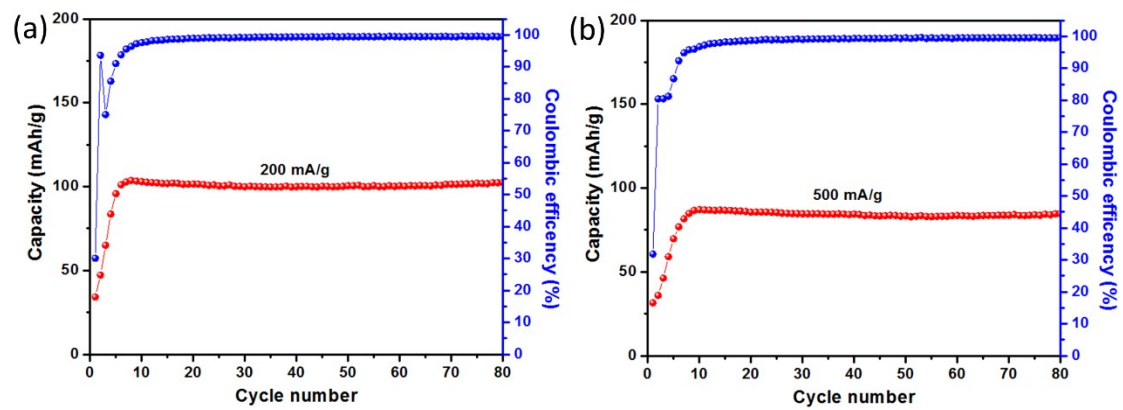


Fig. S10 Cycle performance and the corresponding Coulombic efficiency of carbon black (Super P) (a) at 200 mA/g and (b) at 500 mA/g.

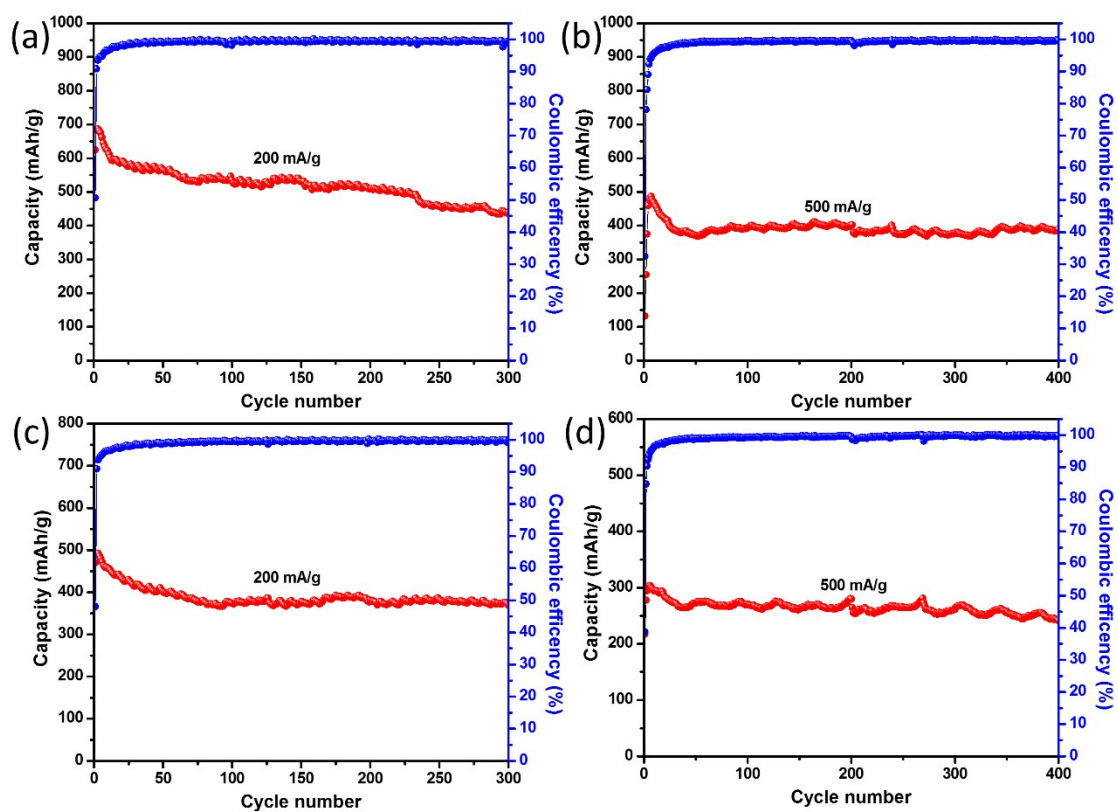


Fig. S11 Cycle performances and the corresponding Coulombic efficiencies of Sn nanoparticles (a and b) and hollow SnO_x nanoparticles (c and d) at 200 mA/g and 500 mA/g after removing capacity contribution of carbon black (Super P).

- 1 X. Zhao, Q. Di, X. Wu, Y. Liu, Y. Yu, G. Wei, J. Zhang and Z. Quan, *Chem. Commun.*, 2017, **53**, 11001-11004.
- 2 A. Bhaskar, M. Deepa and T. N. Rao, *Nanoscale*, 2014, **6**, 10762-10771.